

A 3D-printed soft orthotic hand actuated with twisted and coiled polymer muscles triggered by electromyography signals

Irfan Zobayed^{1,2}, Drew Miles¹, Yonas Tadesse^{1,2,3,4}

¹ Humanoid, Biorobotics, and Smart Systems (HBS) Lab, Mechanical Engineering Department, The University of Texas at Dallas

² Biomedical Engineering Department, The University of Texas at Dallas

³ Electrical and Computer Engineering Department, The University of Texas at Dallas

⁴ Alan G. MacDiarmid Nanotech Institute, The University of Texas at Dallas

ABSTRACT

Various wearable robotic hands, prosthetic hands, and orthotic exoskeletons developed in the last decade aim to rehabilitate patients whose daily quality of life is affected from hand impairments – however, a majority of these devices are controlled by bulky, expensive, noisy, and uncomfortable actuators. Twisted and coiled polymer (TCP) muscles are novel smart actuators that address these key drawbacks. They have been utilized in soft robotics, hand orthosis exoskeletons, and powered hand orthotic devices; they are also light-weight, high-performance, and inexpensive to manufacture. Previously, TCP muscles have been controlled via power supplies with mechanical switches that are not portable, hence making it unfeasible for long term applications. In this work, a portable control system for TCP muscles via electromyography (EMG) signals that are captured through electrodes placed on the arm of the user and processed through a channel of electrical components to actuate 4-ply TCP muscles, which is demonstrated on a 3D-Printed soft orthotic hand. With portable EMG control, orthotic devices can become more independently accessible to the user, making these devices novel instruments for measuring, aiding, and expediting the progress of hand impairment rehabilitation.

Section: RESEARCH PAPER

Keywords: actuators; soft robotics; EMG; rehabilitation measurement instrument; powered hand orthosis

Citation: Irfan Zobayed, Drew Miles, Yonas Tadesse, A 3D-printed soft orthotic hand actuated with twisted and coiled polymer muscles triggered by electromyography signals, Acta IMEKO, vol. 11, no. 3, article 9, September 2022, identifier: IMEKO-ACTA-11 (2022)-03-09

Section Editor: Zafar Taqvi, USA

Received March 15, 2022; **In final form** September 23, 2022; **Published** September 2022

Copyright: This is an open-access article distributed under the terms of the Creative Commons Attribution 3.0 License, which permits unrestricted use, distribution, and reproduction in any medium, provided the original author and source are credited.

Corresponding author: Yonas Tadesse, e-mail: Yonas.Tadesse@utdallas.edu

1. INTRODUCTION

One of the major groups of patients who experience an overall decrease in hand function and ability are those who suffer from ischemic stroke, which makes up for a majority of all strokes suffered worldwide. In fact, the number of strokes that occur annually worldwide is approximately 17 million, justifying why it is one of the most common causes of death in many countries, often trailing coronary artery disease [1]. Specifically in the United States, strokes are the fifth leading cause of death, yielding to more than 125,000 casualties annually as well as leaving long-lasting effects for nearly one million more patients [2]. Alongside the decreased physical ability of patients, strokes also hold a strong economic toll as well, due to health care services, medications, loss of productivity, and required

rehabilitation, which can not only bring economic issues to patients but cost the economy billions of dollars [1].

Worldwide, approximately 50 to 60 million people suffer from some form of hand impairment after suffering not only a stroke but also spinal cord injury (SCI) and skeletal muscle atrophy. This often results in a loss of independence, leading to a decrease in the quality of activities in daily life for such patients [3]. The prevalence of upper-extremity neuromotor impairments because of ischemic strokes and SCI is statistically inevitable – when combined with the economic challenges that come when attempting to manage a stroke, there is an overwhelming issue in access to affordable treatment to treat any related impairments.

Performing rehabilitation on a patient as soon as possible after suffering a stroke gives the best chance of regaining any lost hand functionality and dexterity back to the patient [4]. However, traditional methods of rehabilitation are not only expensive but

also not possible to perform since patients need to be fully conscious and at a minimum state of health post-stroke or injury, which is very uncommon in most cases.

To tackle the expenses and lack of accessibility that comes with rehabilitation for hand impairments, medical robotics have been a refreshing addition to the few options patients have when selecting their path to recovery post-stroke. Specifically, the introduction of powered hand orthotic exoskeletons has made great strides in easing the difficulty that defames neuromotor rehab from both an engineering and clinical perspective. The quality and efficiency of the current common rehabilitation process improvement as well as expediting the overall process that helps retain maximal motor function for patients within the critical period post-stroke. Design parameters for hand exoskeleton devices are imperative to the user experience as well, including a focus on key mechanical aspects that relate to hand anatomy, user comfort, effective force transmission via an actuator, and affordability for the common consumer [5]. The critical combination of such parameters within an exoskeleton device must not only aim to meet user demands but also needs to meet the demands of the industry.

One of the current industry leaders in assistive hand orthotic devices is the MyoPro device that was developed by Myomo Inc. – electromyography, better known as EMG, signals are captured by electrodes upon muscle contractions and filtered through their patented software that is onboard the device itself. The filtered signal then triggers the actuators, which are motors, within the device [6]. Unique due to its combination of portability, self-control mechanism by processing EMG signals, and minimalist look, the MyoPro device exhibits the key combination of design parameters within an exoskeleton device. Although the device can exhibit the dexterity and function of a human hand, the cost to purchase the device for a consumer will yield nearly \$80,000 after insurance, which is unaffordable for a majority of patients who have hand motor impairments. Another industry-leading alternative assistive hand orthotic device is the NASA RoboGlove, a humanoid robotic that was designed to perform and enhance human-scale work, which is an alternative approach to the perspective of rehabilitative applications for stroke patients [7]. The device was developed in a partnership between General Motors and NASA in an attempt to improve and assist healthy humans and their hand mechanical capabilities in applications that may require it, such as performing high-intensity work that requires strength in the International Space Station (ISS) or other zero-gravity environments. Although innovative in its design and application intentions, the RoboGlove is not available to average consumers for purchase, further justifying the need for the accessibility and affordability of hand orthotic devices.

As a result of both the need for affordable soft robotic stroke rehabilitation alternatives and research for accessible optimized combinations of critical parameters for building exoskeletons, there have been multiple attempts to build these devices. Over recent years, there have been many attempts at developing reliable hand orthotic devices, including 165 different separate iterations of dynamic hand orthosis that have been studied and documented by Bos et al. by sifting through 296 different sources of literature, with 109 of the devices developed since 2011. Bos found that a majority of the dynamic hand orthosis is currently powered by DC motors and that devices are powered with traditional power supplies and trigger actuation via manual transmission, force, pressure, pre-tension loads, and in some advanced cases, EMG signals [8].

Several hand orthotic devices are able to perform some of the key functionalities that are presented by the MyoPro and RoboGlove. These hands are much more affordable but are not commercially available. Developed by Butzer et al. is the RELab Tenoexo, which can actuate on spring pre-loaded tension mechanisms via a DC motor that is triggered by processed EMG signals [3]. A similar powered hand orthotic device is also actuated by DC motors that are triggered via EMG signals, which was developed by Park et al. out of Columbia [9]. Another implementation of a hand orthotic device that was partially 3-D printed with PLA filament was developed by Yoo et al., which is also actuated by a DC motor and significantly cheaper than other similar devices.

An overwhelming majority of the devices mentioned as well as other similar devices utilize some form of a traditional or bulky actuator or EMG triggering for the actuation of the device [3], [8], [10]-[14]. Traditional actuators, although affordable, are bulky, noisy, and not user-friendly. A cost-effective, high performance, and lightweight soft artificial actuator called twisted and coiled polymer (TCP) muscles was developed by Haines et al. 2014, who founded a new class of smart actuators that have high power to weight ratios and also alleviate many of the issues that are founded with traditional actuators [15]. TCP muscles are fabricated from precursor fiber conductive multifilament silver-coated nylon 6,6 sewing thread and can exhibit linear strokes as high as 50 % and is easy to both fabricate and manufacture – the first-ever soft robotic powered hand orthotic device to utilize this new class of smart actuators was the iGrab, which is a 3D printed hand orthotic exoskeleton, developed by Saharan et al., that is actuated via 2-ply TCP muscles [16].

Like TCP muscles, other types of smart actuators that also exhibit some of the similar key thermomechanical and electrical properties, which include shape memory alloy (SMA) and fishing line muscles. Both are suitable for various applications given their unique mechanical properties. SMAs are a promising alternative to traditional actuators due to their shape retention abilities when actuating [17]. Furthermore, their muscle-like properties and various methods of cooling them for faster movement prove their relevance in robotic applications [18]. Fishing line muscles (TCP_{FL}) are similar to silver-coated TCP (TCP_{Ag}) muscles in terms of fabrication and manufacturing, but they are developed from a monofilament nylon 6 fishing line rather than a thread, allowing them to produce higher actuation in particular cases, which have been demonstrated in underwater soft robotics [19].

The new class of smart actuators founded by Haines et al. exhibit excellent thermomechanical properties in various soft robotic applications and address most of the key issues that are found within current hand orthotic exoskeleton devices, including affordability and accessibility, as well as user experience, bulky designs, and noisy applications. However, actuation of these muscles was performed manually via a traditional power supply – hence, there is no portable or user-focused method of triggering actuation for them, specifically TCP muscles. As depicted in earlier works related to hand orthotic devices, EMG triggered actuation of DC motors were evaluated and applied to devices, yet no such control exists for TCP muscles. Traditional EMG signal actuation methods utilize advanced signal processing and pattern recognition as discussed by Jafarzadeh et al. [20], who introduces a novel method of EMG signal processing via deep learning with convolutional neural networks (CNN) for more accurate signal processing. A derivation of EMG signal processing from the CNN can be

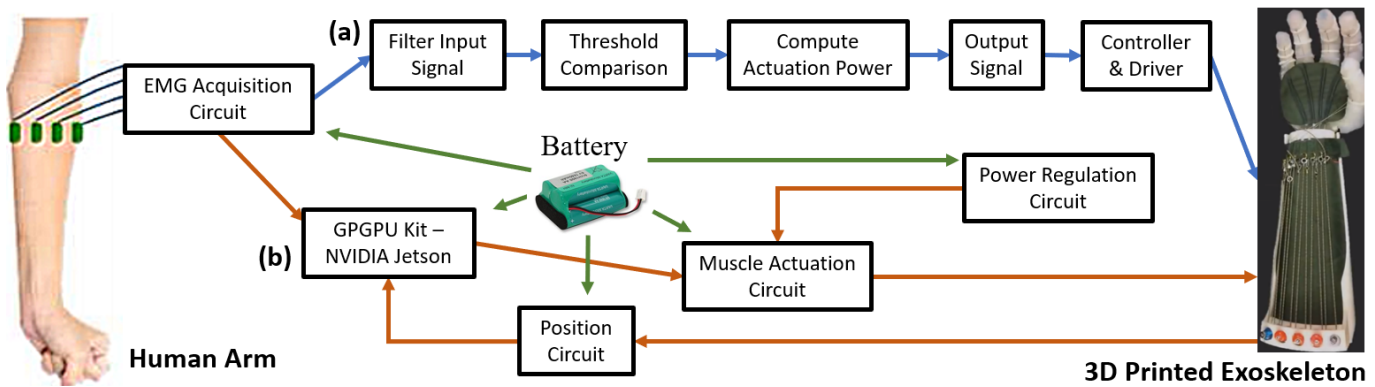


Figure 1. (a) Simplified EMG signal algorithm block diagram (blue arrows) and (b) hardware diagram (orange arrows) for proposed method to control orthotic hands, such as the iGrab hand orthotic device by Lokesh et al. [16], via raw EMG signals.

implemented for accurate EMG results to trigger TCP muscle actuation in a soft robotic application.

In the following study, a novel method of portable TCP muscle control will be introduced, specifically triggering the actuation of these novel smart actuators via processed EMG signals on a 3D printed soft robotic hand and gathering data to evaluate the performance of the system.

2. METHODS & MATERIALS

The following section will thoroughly address the proper methods that were taken place to perform the experimentation and implementation of EMG control of novel artificial TCP muscles concerning the control of a soft robotic, hand orthotic exoskeleton as a complete system as depicted in Figure 1 above.

2.1. TCP Muscle Manufacturing

Twisted and coiled polymer (TCP) muscles are made of precursor fiber conductive multifilament silver-coated nylon 6,6 sewing thread – they can be made as 2-ply, 4-ply, or 6-ply strands, which are each depicted in Figure 2B. The thread can be purchased commercially from Shieldex Trading Inc. in both small cones and large spools. Thicker TCP muscles will require a larger current to actuate as resistance has a direct correlation with length and ply on the muscle [21].

The fabrication of the TCP muscles is prepared in a similar way as described in Saharan et al. [17]. Briefly, a 170 cm long, 200 μm diameter silver-coated nylon fiber strand is cut from the cone or spool – a 2-ply TCP muscle needs 1 strand of fiber; 2 and 3 strands are needed for 4-ply and 6-ply, respectively. The strand(s)

will be connected at each end (2-ply muscles strands are not connected since they are a single thread), which will then have one end attached to a 450 RPM motor and the other end attached to a pre-set load to undergo twist insertion method as seen in Figure 2A. After the fiber strands begin to coil, plying is performed by folding the coiled muscle in half, which will twist in the opposite direction upon release and will then be crimped with a size 6 or 8 gold-plated ring terminal to maintain its shape and tension. The pre-set loads are 175 g, 350 g, and 525 g for 2-ply, 4-ply, and 6-ply muscles, respectively.

For the twisted and plied fibers to actuate properly, electrothermal annealing and training of the TCP muscles are required – each muscle underwent pulse actuation cycles while holding pre-set loads that are slightly heavier than the loads for fabrication – 300 g, 600 g, 900 g are used for 2-ply, 4-ply, and 6-ply, respectively. The exact cycle type, electrical specifications, duration, and repetition that each muscle undergoes are explicitly

Table 1. TCP training cycle specifications.

Step #	Cycle Type	Current (A)			Voltage (V)	Time (s)	# Of Cycles
		2-ply	4-ply	6-ply			
1	Heat	0.7	1.3	2.05	20	10	x6
	Cool	0	0	0	0	45	
2	Heat	0.7	1.3	2.05	20	13	x6
	Cool	0	0	0	0	45	
3	Heat	0.8	1.5	2.3	20	13	x6
	Cool	0	0	0	0	45	
4	Heat	0.8	1.5	2.3	20	15	x15
	Cool	0	0	0	0	45	

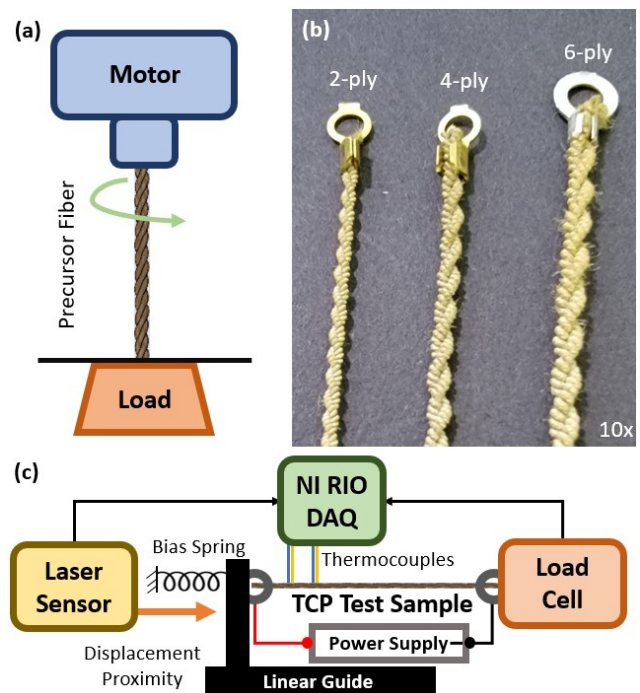


Figure 2. (a) Fabrication set-up for TCP muscles; fibers spun on DC motor at 450 RPM with pre-tension load at the bottom, (b) examples of 2-ply, 4-ply, 6-ply TCP at 10x scale and (c) characterization setup for TCP muscles; the power supply sends current values from steps 3 and 4 of Table 1; NI DAQ device derives temperature from k-type thermocouples, displacement, current, and voltage to calculate the actuation strain and power consumption.

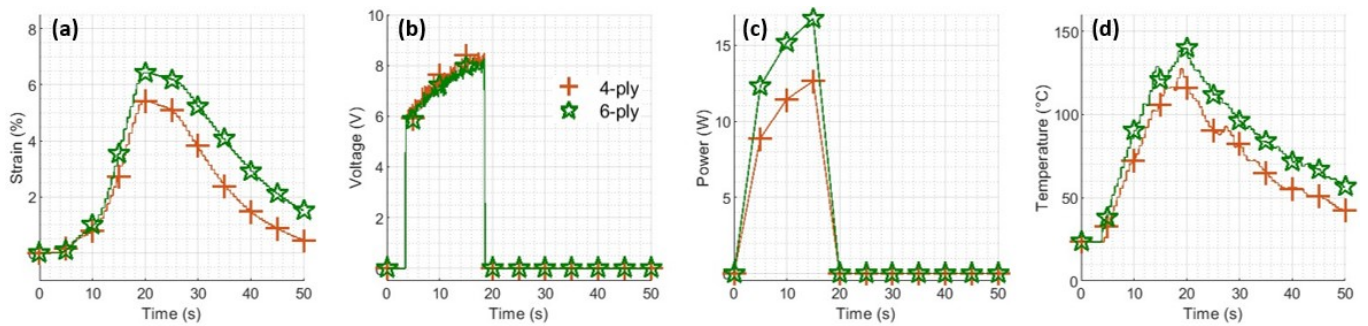


Figure 3. Example characterization data of a 16.7 cm 4-ply and a 17.1 cm 6-ply muscle at 600g for 50 seconds. The current is not depicted since it is a constant input of 1.5 A and 2.1 A for 4-ply and 6-ply, respectively. (a) The strain peaks at 5.5 % for 4-ply and 6.4 % for 6-ply; (b) the voltage peaks at 8.2 V for 4-ply and 8.0 V for 6-ply; (c) the power used peaks at 12.8 W for 4-ply and 16.7 W for 6-ply; (d) the temperature peaks at 129 °C for 4-ply and 140 °C for 6-ply. The number of plies has a direct relationship to the maximum strain a muscle can exhibit.

listed in Table 1. TCP muscles elongate during this process due to the strain placed on the muscle to retain its mechanical properties; the two 4-ply TCP muscles used for this study are ~21.0 cm long post-trained.

To characterize the TCP muscles that are manufactured through the fabrication, training, and annealing phases, the characterization set up, as depicted in Figure 2C, gathers key thermomechanical properties of each muscle placed within the set-up. A single trained TCP muscle is secured onto the set-up platform and has a pre-tension weight added by a defined load cell (300 g, 600 g, and 900 g for 2-ply, 4-ply, and 6-ply muscles respectively). A benchtop power supply then applies a constant current into the muscle, which provides a variable voltage due to the varying resistance of each muscle, hence actuating the TCP muscle. A laser sensor is mounted and secured onto the set up to calculate the displacement of the muscle in real-time when it is actuated. Two thermocouples (Omega, k-type 36 AWG) are attached at two different points on the muscle to follow thermal changes throughout the actuation and cooling process of the muscle. All data from the thermocouples, laser sensor, voltage, and current are captured by a National Instruments (NI) RIO Data Acquisition (DAQ) device, which consisted of an analog output module (NI-9263), differential analog input module (NI-9219), voltage input module (NI-9201), and another single-channel analog input module (NI-9221). The data is then processed into a NI LabVIEW application and outputted into a spreadsheet, whose data is plotted and visualized by an automated MATLAB script for muscle characterization. The data points that are assessed are actuation strain, temperature, current, voltage, and power of each TCP that is manufactured. Actuation results for 4-ply and 6-ply are shown in Figure 3.

All fabrication, training, annealing, and characterization of TCP muscles were performed in the Humanoid, Biorobitics, and Smart Systems (HBS) Laboratory at the Mechanical Engineering Department at The University of Texas at Dallas. For the following article, two fully trained and characterized 4-ply TCP muscles were utilized.

2.2. EMG Signal Algorithm

The algorithm that is depicted in Figure 1A captures raw EMG signals from the electrodes, then filters excess noise and amplifies the raw filtered signal. The input signal then passes through threshold parameters from the electrodes that must be satisfied – these values must be within a certain period of time based on actuation frequencies and between 2 to 3.5 mV for a single finger or 3 to 4.5 mV for two fingers. Once the signal satisfies the threshold, a scaled output signal will be generated to

trigger the controller board, which will communicate to the driver board to send a voltage signal to actuate the 4-ply TCP muscles on the robotic hand.

2.3. EMG Control Setup

The EMG Control set up, depicted in Figure 4, is composed of four main components: the (1) signal acquisition board, (2) power driver control board, (3) sensor data board, and (4) the NVIDIA Jetson TX2 Module controller. For testing purposes, not all board components were connected.

The signal acquisition board, seen in Figure 4D has a total of eight inputs for a maximum of eight electrode pairs and one reference electrode – each electrode pair monitors a different muscle or grouping of muscles. These electrode pairs take raw EMG signals from the subject and send them into the Myoware Muscle Sensor (PN# SEN-13723) seen in Figure 4B and Figure 5A, which will collect the raw EMG signals and input the signal into the board. The Myoware sensor acts in between the electrodes and signal acquisition board.

The power control board, seen in Figure 4E, regulates the voltage and current that is inputted from the battery to power the entire system safely as well as output the voltage to actuate the muscles. The board has a voltage rating of around 20V. The operational amplifiers and DAC chips can output a maximum of 5.7V from each terminal. The board can be fully powered by an operational voltage of only 6V to output an accumulated 45.6V through all eight terminals. The board has a negligible current rating relative to the current it uses. For experimental purposes, a benchtop power supply was utilized in this study.

The sensor data board, seen in Figure 4C, has a total of eight analog inputs to input sensor voltage signals for multiple purposes, including data and performance analytics as well as the implementation of future feedback control systems.

All three boards were designed in Eagle and manufactured by a local PCB vendor. Each board is directly connected to the NVIDIA Jetson TX2, seen in Figure 4A, which acts as the controller and processor for the input data from the sensor data board and power board. The controller was selected for its ability to filter copious quantities of data within the EMG processing algorithm for multiple fingers and output proper commands to the power control board to output the necessary voltage and current to move the hand orthotic device from its pre-trained position to the desired position seen in Figure 5E and in Figure 5F.

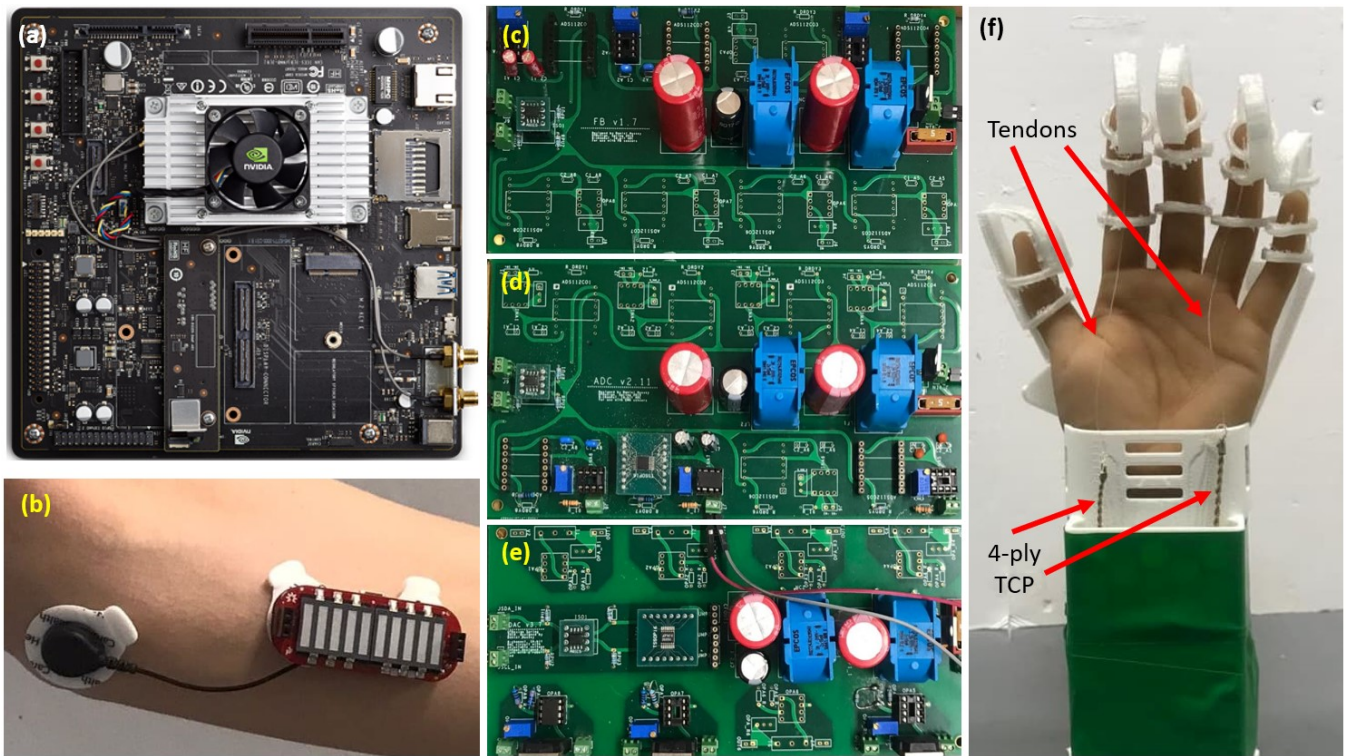


Figure 4. The components that power the EMG triggered actuation system consists of the (a) NVIDIA Jetson TX2, (b) Myoware muscle sensor, (c) sensor data board, (d) signal acquisition board, (e) power control board, and (f) a 3-D printed orthotic hand, which is actuated by 4-ply TCP muscles connected by a commercial fishing line tendon to each the index and ring finger.

2.4. Orthotic Hand

Depicted in Figure 4F, the 3-D printed orthotic hand is a prototype developed in-house and was set up as a testing apparatus for experimental purposes. The material of the 3-D printed hand orthotic device is made of Thermoplastic

polyurethane (TPU) material and is actuated by two 21 cm post-trained 4-ply TCP muscles, which are each connected to the index finger and ring finger of the orthotic hand by commercial fishing line that will mimic the anatomical functionality of a tendon in the human hand.

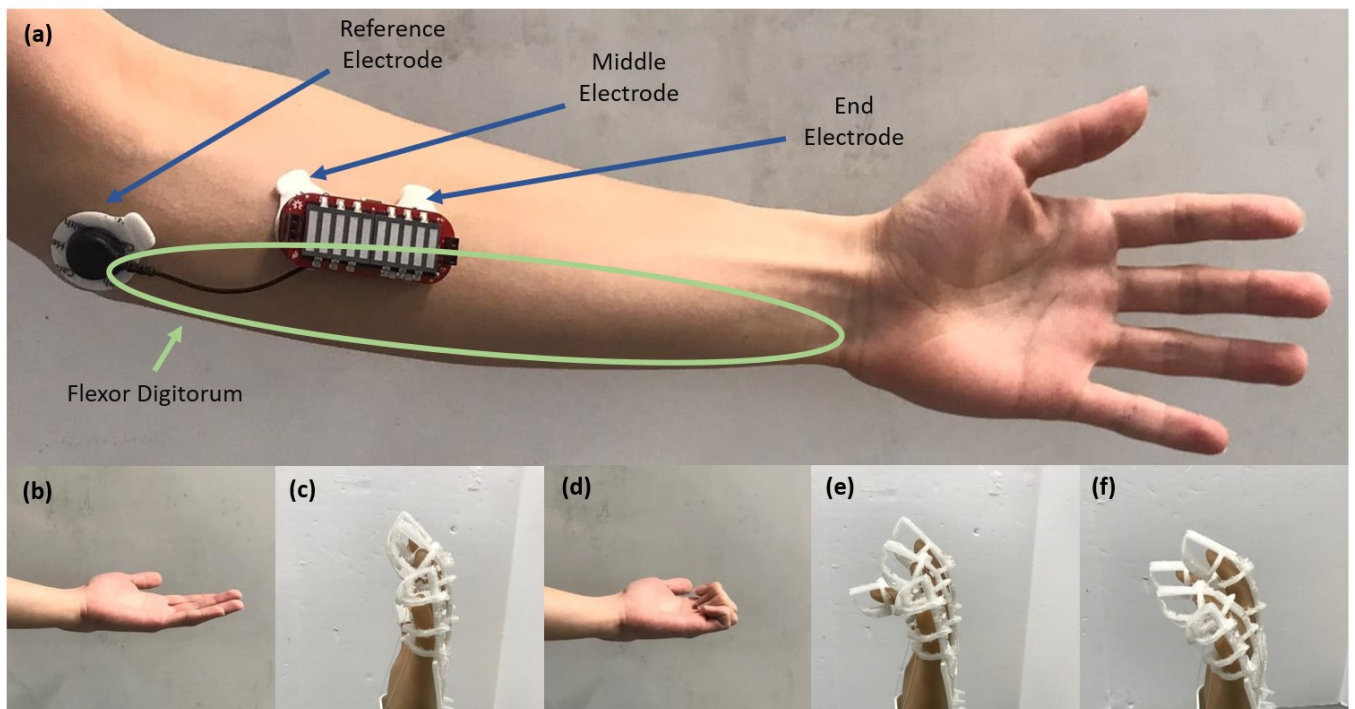


Figure 5. (a) Electrode placement used for EMG controlled actuation in relation to key anatomical muscle structure of the anterior left forearm for clear signal reception; (b) an open hand, which is the rest position for the user, will not actuate the hand and keep the (c) device in its pre-trained rest position; (d) a curled of closed hand by the user will trigger a signal to actuate the TCP muscles, which (e) actuates the ring finger or (f) both the ring and index finger.

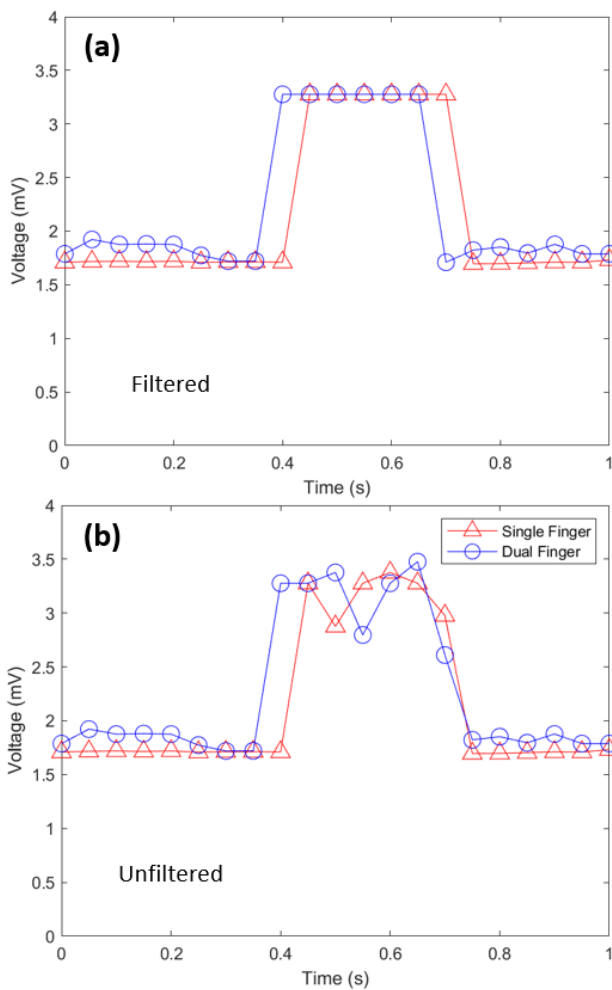


Figure 6. The EMG acquisition signals depicted are a result of the raw EMG signals captured by the three electrodes on the Myoware muscle sensor, which were filtered and adjusted by the controller; (a) filtered EMG signals and (b) unfiltered EMG signals.

2.5. Test Subject

To trigger actuation of the hand orthotic device via EMG signals, a verified subject was required, hence an Institutional Review Board or IRB approval was applied for and granted. Electrodes from the EMG control setup were placed on the anterior surface of the subjects' arm at the base of the forearm, distal to the elbow joint with a reference on the medial bony protrusion of the elbow. The muscle of primary interest is the flexor digitorum profundus, shown in Figure 5A.

3. RESULTS

The following section depicts the results of the experimentation conducted for the actuation of a single finger and dual finger setup, as well as a brief overview of the muscle performance and potential areas of experimental improvement for the data seen in Figure 6.

3.1. Single Finger Actuation

Depicted in Figure 6A is the acquisition of the filtered EMG signal, denoted by the red-triangle-line for a single finger set-up. Initially reading a voltage of 1.72 mV from the electrode while the user was in rest position (seen in Figure 5B), the user then closed their hand (seen in Figure 5D), yielding a spike in voltage to 3.42 mV for a duration of 0.35 seconds and causing the

orthotic hand to also close before returning to a steady voltage around 1.72 mV in rest position. The full flexion yielded from the actuation strain is depicted by the index finger seen on the orthotic hand in Figure 5E. The output voltage from the power control board to the muscle was ~ 5.8 V, which was expected given the electrical specifications of the board and verified with a multimeter. In Figure 6B, the acquisition of the single finger unfiltered EMG signal that was processed by the Myoware muscle sensor is depicted, showing a similar trend to that of the filtered signal.

3.2. Dual Finger Actuation

Portrayed in Figure 6A is the acquisition of the filtered EMG signal for a double finger set-up, denoted by the blue-circle-line. Similar to the single finger, the initial voltage when the user's hand was at rest was at 1.78 mV before the user closed their hand, which then yielded a spike in the filtered voltage to 3.42 mV for a duration of 0.35 seconds before returning to a steady voltage around 1.74 mV. The full flexion of the two fingers, which were observed on the index finger and ring finger simultaneously, is depicted in Figure 5F, which were both connected via the same set-up seen in the single finger set-up for both fingers. In Figure 6B, the acquisition of the dual finger unfiltered EMG signal that was processed by the Myoware muscle sensor is depicted, showing a similar trend to that of the filtered signal.

3.3. Signal Comparison

When plotted side by side, the filtered EMG signals that were acquired from the electrode on the user, which are seen in Figure 6A, depict similar shapes and trends – the same can be said for the side-by-side comparison of the unfiltered signals depicted in Figure 6B. When comparing the statistical data discussed earlier in this section, there are similar power sources of voltage from the electrode, which should be expected given that the same hand gestures were performed. This verifies that the EMG input is acquired correctly by the signal acquisition board and converted properly by the microprocessor because the output voltage from the power control board was able to reach peak voltage for a maximum actuation strain and flexion.

It is important to note that during the rest phases (before the initial spike of the voltage at 0.4s and 0.35s for single and dual finger set-ups, respectively) that for the two different set-ups, it is evident that the EMG voltage of the dual finger set-up has a very slight variance when compared to that of the single finger set-up – this is because there are two output channels opened from the power control board for the actuation of the orthotic hand.

As more channels are opened, the filtering of the acquisition signal from the electrodes becomes slightly weaker, causing the variation seen for the dual finger actuation. Although there is the presence of a slight variance, it is not enough to determine a significant impact on the acquisition and filtering of the signals. Furthermore, the signals acquired are solely that of the subject approved via the IRB process and no one else, as EMG signals can vary amongst each individual, commonly ranging between 1 mV to 10 mV, which is comfortably within the range of acquisition seen in the study [22]. Additional subject tests will optimize the current acquisition and filtration algorithm.

3.4. Response Time

The single finger actuation began 0.4 seconds from the initial start of the EMG signal capture whereas the dual finger actuation began 0.05 seconds earlier at 0.35 seconds. Although the

response time is faster as the number of open channels increase, studies with more actuated fingers should be performed to validate this relationship. Further improvements to the current raw signal capture methods can also improve response time. However, the response time of the TCP muscle is slower due to the time it needs to cool, which is a typical behaviour of thermal muscles (See Figure 3A).

3.5. Performance

The muscles perform with a delayed actuation producing an assistive push to the orthotic hand, approximately 0.4 seconds for the single finger actuation and 0.35 seconds for the dual finger actuation. Through coupling with muscles on the posterior side of the arm, movement will become slower, smoother, and have a higher degree of control. Drawing from the conclusions seen in previous studies [17], the utilization of 2-ply muscles instead of 4-ply would increase the speed of actuation with lesser power consumption but might not be strong enough to further develop into a compact device. Likewise, 6-ply muscles would have the necessary strength (as seen by the example muscles in Figure 3) to actuate but will require greater than the 5.7 volts provided in the current experiment. Furthermore, testing more channels might allow for further insight into variations of the EMG signal acquisition, which can then be addressed by updating the current processing and filtering algorithm.

4. DISCUSSION

TCP muscles are a quality candidate for an effective low-cost orthotic device. The muscles used in this device were of short length without a pulley system, hence resulting in a much shorter strain per actuation with a higher degree of precision and control. If the individual muscles were combined with many others similar to that of human muscles, smoother and more powerful motion could be obtained. The performance of these muscles is also affected by the power limitations of the board. While TCP muscles perform optimally at around 6-13 V depending on the specific ply, the highest deliverable voltage with the current set-up design is approximately 5.7 V [20].

SMA muscles can perform well at the provided voltage but increase the production cost greatly and potential hysteresis during the cooling process can also slow down the efficiency of actuation. Fishing line muscles are another powerful soft artificial muscle that actuates based on temperature changes. The heating and cooling of these muscles can be achieved through water or fans depending on the size and containment of the system [17], [23]. However, the amount of actuation currently produced is not inherently undesirable for an assistive motion and the following study supports that this motion can be increased temporarily for the rehabilitation phase of product use.

An important distinction is the degree and type of care needed for rehabilitation versus assistance in daily activities. Robotic devices have been used in research studies for motor function rehabilitation quite extensively in the past twenty years. These training periods typically last around one hour and are conducted with at least one day between each session [24]. Assistive devices are designed to be worn during all hours of daily life to assist with essential tasks and functions. Once a person's functionality is restored to their individual peak, an assistive device works to fill the gaps between their current functionality and their pre-incident functionality [25], which can potentially become more accessible to patients as more iterations of portable and soft orthotic hand devices are investigated.

The performance of this device in its current form has not yet been determined through standard human subject tests. This is appropriate as the initial tests performed verified the efficacy and need for further testing through credited existing tests. The Fugl Meyer test is a classic functionality test that examines the degree of functionality that a person possesses in their upper extremities [26]. When performed with and without an assistive device, the respective scores can be compared to assess the effectiveness of the device. Additional tests such as the Action Research Arm Test (ARAT), Wolf Motor Test, and Box and Block Test can provide a more holistic characterization of soft robotic assistive device performance [27]-[29].

EMG controlled actuation, through soft or hard actuators, requires precise processing and filtering of the EMG signal in real-time. The methods required for such processing depend on the system used for EMG acquisition, the muscles being monitored, and the sensor used. The EMG acquisition of the flexor digitorum profundus results in desirable levels of control for hand orthotic devices [30]. This could be improved through the addition of a complementary sensor placed on the posterior surface of the forearm in the same position as the original sensor. Likewise, the addition of further processing techniques can serve as an alternative to additional electrode placement [31]. Such research can be performed and further investigated from the given study, potentially enabling the development of more novel solutions that are tailored to both affordability and accessibility of the device for patients as well as thorough user experience.

5. CONCLUSION

Loss of hand movement or functionality is a widespread problem in the world today. The orthotic hand discussed would restore functionality to the user at a fraction of the cost of currently available systems. Furthermore, it can be utilized a measurement tool for rehabilitative progress for patients who are trying to regain functionality in their hand.

With human subject trials, the device can be further improved for better portability and convenience. Additional testing will also yield more EMG data, allowing for more precise control of the device. Integrating existing gesture-based EMG databases with our current algorithms will allow for complex mechanical movements of the orthotic device [32]. This same technology can apply not only well to low-cost prosthetics and rehabilitative robotics for trans-ulnar amputees, but also as assistive devices for the general use of able-bodied individuals [33]. With modifications, this technology could have useful applications for restoring functionality in those with Parkinson's disease or who suffer from foot drops. The orthotic device discussed has immense potential to positively impact the daily lives of thousands of individuals across the world from not only a functionality perspective but also that of an instrument to measure rehabilitative progress.

6. FUNDINGS

The following research was supported by internal source research enhancement.

7. COMMENTS

The authors declare no conflicts of interest. This paper is the full version of the presentation "iGrab: Novel 3D printed Soft Orthotic Hand Triggered by EMG signals" presented at the TC17 Special Events Conference in October 2021.

REFERENCES

- [1] B. R. French, R. S. Boddepalli, R. Govindarajan, Acute Ischemic Stroke: Current Status and Future Directions, *Mo. Med.*, vol. 113, no. 6, pp. 480–486, 2016. Online [Accessed 27 September 2022] <https://www.ncbi.nlm.nih.gov/pmc/articles/PMC6139763/>
- [2] S. L. Murphy, K. D. Kochanek, J. Xu, E. Arias, Mortality in the United States, 2020, 2021. Online [Accessed 27 September 2022] <https://pubmed.ncbi.nlm.nih.gov/34978528/>
- [3] T. Bützer, O. Lambercy, J. Arata, R. Gassert, Fully wearable actuated soft exoskeleton for grasping assistance in everyday activities, *Soft Robot.*, vol. 8, no. 2, pp. 128–143, 2021. DOI: [10.1089/soro.2019.0135](https://doi.org/10.1089/soro.2019.0135)
- [4] P. Langhorne, J. Bernhardt, G. Kwakkel, Stroke rehabilitation, *The Lancet*, vol. 377, no. 9778, pp. 1693–1702, 2011. DOI: [10.1016/S0140-6736\(11\)60325-5](https://doi.org/10.1016/S0140-6736(11)60325-5)
- [5] M. Sarac, M. Solazzi, A. Frisoli, Design requirements of generic hand exoskeletons and survey of hand exoskeletons for rehabilitation, assistive, or haptic use, *IEEE Trans. Haptics*, vol. 12, no. 4, pp. 400–413, 2019. DOI: [10.1109/TOH.2019.2924881](https://doi.org/10.1109/TOH.2019.2924881)
- [6] J. P. McCabe, D. Henniger, J. Perkins, M. Skelly, C. Tatsuoka, S. Pundik, Feasibility and clinical experience of implementing a myoelectric upper limb orthosis in the rehabilitation of chronic stroke patients: a clinical case series report, *PloS One*, vol. 14, no. 4, p. e0215311, 2019. DOI: [10.1371/journal.pone.0215311](https://doi.org/10.1371/journal.pone.0215311)
- [7] C. A. Ihrke, L. B. Bridgwater, D. R. Davis, D. M. Linn, E. A. Laske, K. G. Ensley, J. H. Lee, RoboGlove-A robonaut derived multipurpose assistive device, 2014.
- [8] R. A. Bos, C. J. W. Haarman, T. Stortelder, K. Nizamis, J. L. Herder, A. H. A. Stienen, D. H. Plettenburg, A structured overview of trends and technologies used in dynamic hand orthoses, *J. Neuroengin. Rehabil.*, vol. 13, no. 1, 2016, pp. 1-25. DOI: [10.1186/s12984-016-0168-z](https://doi.org/10.1186/s12984-016-0168-z)
- [9] S. Park, M. Fraser, L. M. Weber, C. Meeker, L. Bishop, D. Geller, J. Stein, Matei Ciocarlie User-driven functional movement training with a wearable hand robot after stroke, *IEEE Trans. Neural Syst. Rehabil. Eng.*, vol. 28, no. 10, pp. 2265–2275, 2020. DOI: [10.1109/TNSRE.2020.3021691](https://doi.org/10.1109/TNSRE.2020.3021691)
- [10] L. Randazzo, I. Iturrate, S. Perdikis, J. d R. Millán, mano: A wearable hand exoskeleton for activities of daily living and neurorehabilitation, *IEEE Robot. Autom. Lett.*, vol. 3, no. 1, pp. 500–507, 2017.
- [11] T. Shahid, D. Gouwanda, S. G. Nurzaman, Moving toward soft robotics: A decade review of the design of hand exoskeletons, *Biomimetics*, vol. 3, no. 3, p. 17, 2018. DOI: [10.3390/biomimetics3030017](https://doi.org/10.3390/biomimetics3030017)
- [12] T. du Plessis, K. Djouani, C. Oosthuizen, A review of active hand exoskeletons for rehabilitation and assistance, *Robotics*, vol. 10, no. 1, p. 40, 2021.
- [13] N. Secciani, C. Brogi, M. Pagliai, F. Buonomici, F. Gerli, F. Vannetti, M. Bianchini, Y. Volpe, A. Ridolfi, Wearable Robots: An Original Mechatronic Design of a Hand Exoskeleton for Assistive and Rehabilitative Purposes, *Front. Neurorobotics*, vol. 15, 2021. DOI: [10.3389/fnbot.2021.750385](https://doi.org/10.3389/fnbot.2021.750385)
- [14] P. Heo, G. M. Gu, S. Lee, K. Rhee, J. Kim, Current hand exoskeleton technologies for rehabilitation and assistive engineering, *Int. J. Precis. Eng. Manuf.*, vol. 13, no. 5, pp. 807–824, 2012.
- [15] C. S. Haines (+ 20 authors), Artificial muscles from fishing line and sewing thread, *science*, vol. 343, no. 6173, pp. 868–872, 2014. DOI: [10.1126/science.1246906](https://doi.org/10.1126/science.1246906)
- [16] L. Saharan, M. J. de Andrade, W. Saleem, R. H. Baughman, Y. Tadesse, iGrab: hand orthosis powered by twisted and coiled polymer muscles, *Smart Mater. Struct.*, vol. 26, no. 10, p. 105048, 2017.
- [17] L. Wu, M. Jung de Andrade, R. Rome, C. Haines, M. D. Lima, R. H. Baughman, Y. Tadesse, Nylon-muscle-actuated robotic finger, in *Active and Passive Smart Structures and Integrated Systems* 2015, 2015, vol. 9431, pp. 154–165. DOI: [10.1117/12.2084902](https://doi.org/10.1117/12.2084902)
- [18] Y. Tadesse, N. Thayer, S. Priya, Tailoring the response time of shape memory alloy wires through active cooling and pre-stress, *J. Intell. Mater. Syst. Struct.*, vol. 21, no. 1, pp. 19–40, 2010.
- [19] Y. Almubarak, M. Schmutz, M. Perez, S. Shah, Y. Tadesse, Kraken: A wirelessly controlled octopus-like hybrid robot utilizing stepper motors and fishing line artificial muscle for grasping underwater, 2021. DOI: [10.21203/rs.3.rs-186985/v1](https://doi.org/10.21203/rs.3.rs-186985/v1)
- [20] M. Jafarzadeh, D. C. Hussey, Y. Tadesse, Deep learning approach to control of prosthetic hands with electromyography signals, in *2019 IEEE International Symposium on Measurement and Control in Robotics (ISMCR)*, 2019, pp. A1-4. DOI: [10.1109/ISMCR47492.2019.8955725](https://doi.org/10.1109/ISMCR47492.2019.8955725)
- [21] I. M. Zobayed, Y. Tadesse, iGrab: Mechanical characterization of 4-ply and 6-ply TCP muscle actuators for Hand Orthotic Exoskeleton. *Biomedical Engineering Society (BMES) Annual Meeting*, (poster). October 6-9. Orlando, FL.
- [22] M. B. I. Reaz, M. S. Hussain, F. Mohd-Yasin, Techniques of EMG signal analysis: detection, processing, classification and applications, *Biol. Proced. Online*, vol. 8, no. 1, pp. 11–35, 2006.
- [23] L. Saharan, Y. Tadesse, A novel design of thermostat based on fishing line muscles, in *ASME International Mechanical Engineering Congress and Exposition*, 2016, vol. 50688, p. V014T07A019. DOI: [10.1115/IMECE2016-67298](https://doi.org/10.1115/IMECE2016-67298)
- [24] A. C. Lo (+ 19 authors), Robot-assisted therapy for long-term upper-limb impairment after stroke, *N. Engl. J. Med.*, vol. 362, no. 19, pp. 1772–1783, 2010. DOI: [10.1056/nejmoa0911341](https://doi.org/10.1056/nejmoa0911341)
- [25] B. Radder (+ 9 authors), A wearable soft-robotic glove enables hand support in ADL and rehabilitation: a feasibility study on the assistive functionality, *J. Rehabil. Assist. Technol. Eng.*, vol. 3, p. 2055668316670553, 2016. DOI: [10.1177/2055668316670553](https://doi.org/10.1177/2055668316670553)
- [26] D. J. Gladstone, C. J. Danells, S. E. Black, The Fugl-Meyer assessment of motor recovery after stroke: a critical review of its measurement properties, *Neurorehabil. Neural Repair*, vol. 16, no. 3, pp. 232–240, 2002.
- [27] M. McDonnell, Action research arm test, *Aust J Physiother*, vol. 54, no. 3, p. 220, 2008. DOI: [10.1016/S0004-9514\(08\)70034-5](https://doi.org/10.1016/S0004-9514(08)70034-5)
- [28] E. Taub, D. M. Morris, J. Crago, Wolf motor function test (WMFT) manual, *Birm. Univ. Ala. CI Ther. Res. Group*, pp. 1–31, 2011.
- [29] T. Platz, C. Pinkowski, F. van Wijck, I.-H. Kim, P. Di Bella, G. Johnson, Reliability and validity of arm function assessment with standardized guidelines for the Fugl-Meyer Test, *Action Research Arm Test and Box and Block Test: a multicentre study*, *Clin. Rehabil.*, vol. 19, no. 4, pp. 404–411, 2005. DOI: [10.1191/0269215505cr832oa](https://doi.org/10.1191/0269215505cr832oa)
- [30] M. Mulas, M. Folgheraiter, G. Gini, An EMG-controlled exoskeleton for hand rehabilitation, in *9th International Conference on Rehabilitation Robotics*, 2005. ICORR 2005., 2005, pp. 371–374. DOI: [10.1109/ICORR.2005.1501122](https://doi.org/10.1109/ICORR.2005.1501122)
- [31] H.-J. Yoo, S. Lee, J. Kim, C. Park, B. Lee, Development of 3D-printed myoelectric hand orthosis for patients with spinal cord injury, *J. Neuroengineering Rehabil.*, vol. 16, no. 1, pp. 1–14, 2019. <https://jneuroengrehab.biomedcentral.com/articles/10.1186/s12984-019-0633-6>
- [32] N. J. Jarque-Bou, M. Vergara, J. L. Sancho-Bru, V. Gracia-Ibáñez, and A. Roda-Sales, A calibrated database of kinematics and EMG of the forearm and hand during activities of daily living, *Sci. Data*, vol. 6, no. 1, pp. 1–11, 2019. <https://www.nature.com/articles/s41597-019-0285-1>
- [33] S. Park, C. Meeker, L. M. Weber, L. Bishop, J. Stein, M. Ciocarlie, Multimodal sensing and interaction for a robotic hand orthosis, *IEEE Robot. Autom. Lett.*, vol. 4, no. 2, pp. 315–322, 2018.